



Biomass, production, and control of heterotrophic bacterioplankton during a late phytoplankton bloom in the Amundsen Sea Polynya, Antarctica



Jung-Ho Hyun^{a,*}, Sung-Han Kim^a, Eun Jin Yang^b, Ayeon Choi^a, Sang Hoon Lee^b

^a Department of Marine Sciences and Convergent Technology, Hanyang University, 55 Hanyangdaehak-ro, Sangnok-gu, Ansan, Gyeonggi-do 15588, Republic of Korea

^b Division of Polar Climate Research, Korea Polar Research Institute, Incheon 406-840, Republic of Korea

ARTICLE INFO

Available online 17 October 2015

Keywords:

Bacterial production
Microbial loop
Amundsen Sea
Polynya
Phaeocystis bloom

ABSTRACT

We investigated the heterotrophic bacterial biomass and production in February 2012, in four habitats (a polynya, sea-ice zone, ice shelf, and the open sea) in the Amundsen Sea to determine the spatial distribution, controlling factors, and ecological role of the bacteria during a late phytoplankton bloom by *Phaeocystis antarctica*. Bacterial abundance (BA) and production (BP) were highest at the center of the polynya, and both were significantly correlated with phytoplankton biomass. BP accounted for average 17% of the organic carbon produced by phytoplankton primary production (PP), which is higher than the average BP:PP ratio reported in most open ocean. The abundance of heterotrophic nanoflagellates (HNF) was correlated with the BA, and the average bacteria:HNF ratio (260) was lower than the values reported in most marine environments (400–1000), including the Ross Sea Polynya (800). Evidence for a tight coupling of bacteria and phytoplankton activities on the one hand and intense HNF grazing on bacteria on the other could be found in the high BP:PP and low bacteria:HNF ratios, respectively. Interestingly, these data were accompanied by low particulate carbon export fluxes measured during the late *Phaeocystis* bloom. Together, these results indicated that the microbial loop plays a significant role in the biogeochemical carbon cycle and food web processes in the Amundsen Sea Polynya.

© 2015 Elsevier Ltd. All rights reserved.

1. Introduction

Heterotrophic prokaryotes (hereafter bacteria, as the traditional ecological term) are a significant biological controlling factor in biogeochemical carbon cycles in the water column (Kirchman, 2008). Heterotrophic bacteria directly metabolize or contribute to the solubilization of sinking and suspended particulate organic carbon (POC), and are responsible for the rapid turnover of dissolved organic carbon (DOC) from various sources (Carlson, 2002; Nagata, 2008). The DOC assimilated by the bacteria is then either transferred to higher trophic levels via the microbial loop (Azam et al., 1983; Sherr et al., 1988) or respired to CO₂ (Ducklow et al., 1986; del Giorgio et al., 1997), which determines the role of the microbial loop in biogeochemical carbon cycles and the efficiency of the biological pump or export flux (Legendre and Fèvre, 1995). Therefore, it is essential to quantify bacterial parameters such as biomass, production, and respiration, and their controlling factors in time and space to construct models for biogeochemical carbon

cycles and microbial food web processes at the local or global scale (Ducklow, 2000; del Giorgio and Williams, 2005).

The coastal zone of the Southern Ocean is typically characterized by the occurrence of polynyas; i.e., areas of seasonally recurring open water surrounded by sea-ice (Williams et al., 2007; Nihashi and Ohshima, 2015). Due to the combined effects of the enhanced light conditions, supply of Fe, and formation of stratified conditions resulting from melting sea-ice, polynyas are among the most productive marine ecosystems (Sedwick and DiTullio, 1997; Smith and Gordon, 1997; Arrigo and van Dijken, 2003; Montes-Hugo and Yuan, 2012), and thus are regarded as significant sources of biogenic gases and as a sink for atmospheric CO₂ (Miller and DiTullio, 2007; Arrigo et al., 2008). Therefore, it is particularly important to determine the role of heterotrophic bacteria that are associated with the fate of primary production (PP) in highly productive polynyas and continental shelves in the Southern Ocean, where rapid warming and glacial ice melting occurs (Ducklow and Yager, 2006; Kirchman et al., 2009).

The Amundsen Sea is located in western Antarctica between the Ross Sea and Bellingshausen Sea (69°S–74°S; 100°W–135°W, Fig. 1), and is characterized by a large polynya from November to February

* Corresponding author.

E-mail address: hyunjh@hanyang.ac.kr (J.-H. Hyun).

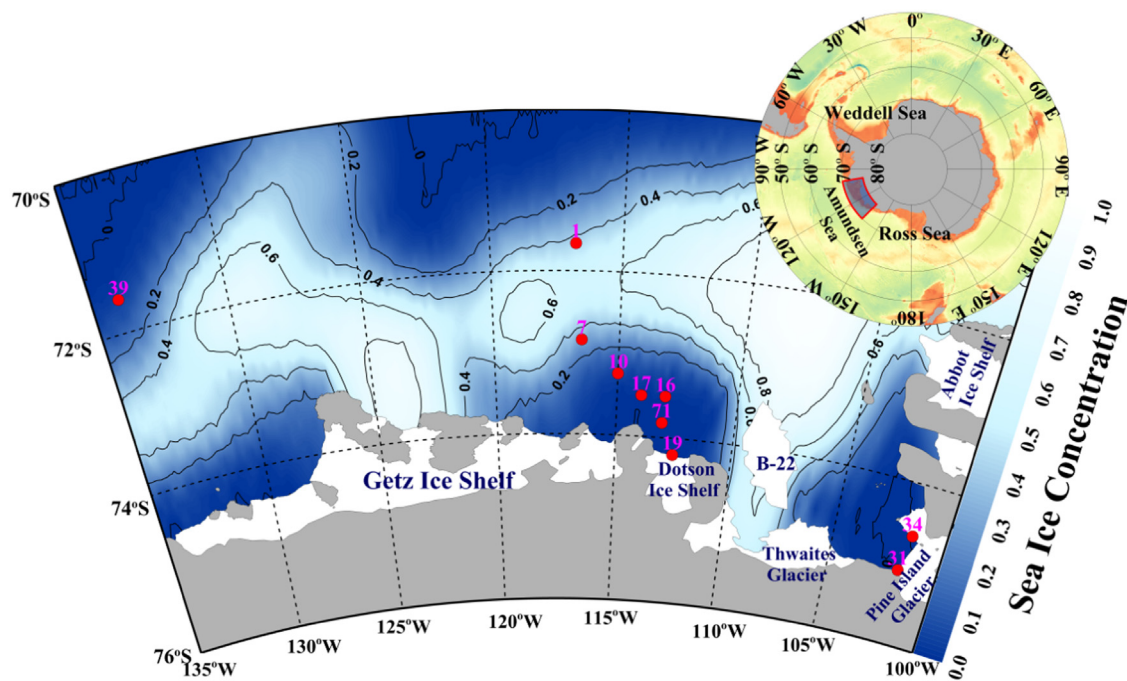


Fig. 1. Map of study area showing sampling stations and average sea ice concentration in February, 2012. Contour lines indicate sea ice concentration. Average sea ice concentration data was obtained from the Nimbus-7 Scanning Multichannel Microwave Radiometer (SMMR, 1979–1987), the Defense Meteorological Satellite Program (DMSP) Special Sensor Microwave/Imager (SSM/I, 1987–2007) and the Special Sensor Microwave Imager/Sounder (SSMIS, 2008–present) (Cavalieri et al., 1996).

(Arrigo and van Dijken, 2003). Satellite images show that the Amundsen Sea has experienced significant surface warming and loss of sea-ice (Jacobs et al., 1996; Jenkins et al., 1997; Stammerjohn et al., 2008; Thoma et al., 2008). The glaciers near the Amundsen Sea are undergoing the highest rates of melting and thinning in the Antarctic continent (Rignot, 2008; Schoof, 2010). The inflow of warm Circumpolar Deep Water (CDW) that eventually upwells underneath the Pine Island Glacier (PIG), Getz Ice Shelf and Dotson Ice Shelf is the main cause of the increased rate of glacier melt in the Amundsen Sea (Jenkins et al., 2010; Jacobs et al., 2011). Since the glacial meltwater contains high Fe (Poulton and Raiswell, 2005), the melting ice provides an ideal condition for phytoplankton blooms within the coastal polynya during the spring and summer (Alderkamp et al., 2012; Fragoso and Smith, 2012; Gerringa et al., 2012). As a result, the Amundsen Sea Polynya (ASP) is reported to be the most productive of the 37 coastal polynyas around Antarctica (Arrigo and van Dijken, 2003; Arrigo et al., 2012) with the highest PP per unit area, ranging from 175 to 220 $\text{g C m}^{-2} \text{y}^{-1}$ (Lee et al., 2012; Kim et al., 2014a). Although several microbiological studies have been conducted in various polynyas in the Arctic and Antarctic oceans (e.g., Ducklow and Yager, 2006), little is known about the bacterial dynamics in the ASP (Yager et al., 2012; Kim et al., 2014b; Delmont et al., 2014). The main objectives of this study were: (1) to identify the spatial distribution of bacterial abundance (BA) and bacterial production (BP) along the continental shelf, polynya and ice shelf of the Amundsen Sea; (2) to elucidate the factors controlling BA and BP; and (3) to evaluate the significance of the microbial loop during a late bloom of *Phaeocystis antarctica* in the ASP.

2. Materials and methods

This study was conducted during a Korean Amundsen Sea expedition on board the icebreaker R/V Araon from February 9 to March 10 in 2012. Earlier studies in the ASP reported that the highest phytoplankton biomass occurs in January–February, and the bloom declines quickly in late February–early March (Arrigo and van Dijken,

2003). The average chlorophyll-*a* (Chl *a*) concentration and PP in January has been reported as 395 mg m^{-2} and 2.2 $\text{g C m}^{-2} \text{day}^{-1}$, respectively, (Lee et al., 2012), but declined to 65 mg m^{-2} and 0.25 $\text{g C m}^{-2} \text{d}^{-1}$, respectively, in February (Kim et al., 2014a). Therefore, our sampling period was regarded as a late bloom condition. Size-fractionated analysis of Chl *a* concentration also revealed that large phytoplankton (> 20 μm), mostly *Phaeocystis antarctica*, were the most dominant phytoplankton communities, comprising more than 60% of total Chl *a* (Lee et al., 2012; Kim et al., 2014a). Four representative sites were selected along the marginal sea-ice zone in the outer shelf (Stns 1 and 7), the polynya (Stns 10, 16, 17 and 71), the ice shelf region (Stns 19, 31 and 34), and an open sea site (Stn 39) in the Amundsen Sea (Fig. 1). In order to examine the dependence of BP on DOC, we re-visited the center of the polynya in March (i.e., Stn 17-1; measurements from February are denoted as Stn 17, whereas those from March are denoted as Stn 17-1, Figs. 2 and 3).

2.1. Physico-chemical parameters

Temperature and salinity were measured using a conductivity-temperature-depth (CTD) probe (SBE 911 Plus, Seabird Electronics). Seawater samples for chemical and biological analyses were collected from depths of 100, 70, 60, 40–50, 30, 10, and 1 m using Niskin bottles attached to a rosette sampler. The sample bottles were first washed with 10% HCl and rinsed with Milli-Q water. The Chl *a* concentration was determined using a fluorometer (Turner Designs Trilogy) after filtration through GF/F filters (0.7 μm pore size) (Parsons et al., 2005). In addition, *in situ* Chl *a* fluorescence was measured using an underwater fluorometer (SeaTech) to depict the vertically continuous distributions of Chl *a*. The Chl *a* concentrations were then calculated from the linear relationship between the *in situ* fluorescence (flu) and the spectrophotometrically measured concentrations of Chl *a*; $\text{Chl } a = 0.644 \times \text{flu} + 0.549$ ($r^2 = 0.86$, $n = 49$).

Samples used to measure chromophoric dissolved organic matter (CDOM) were filtered through a syringe filter (Advantec, pore size 0.2 μm) that had been pre-washed with ultra-pure Milli-Q water, and then stored in 150 mL amber bottles in the dark at

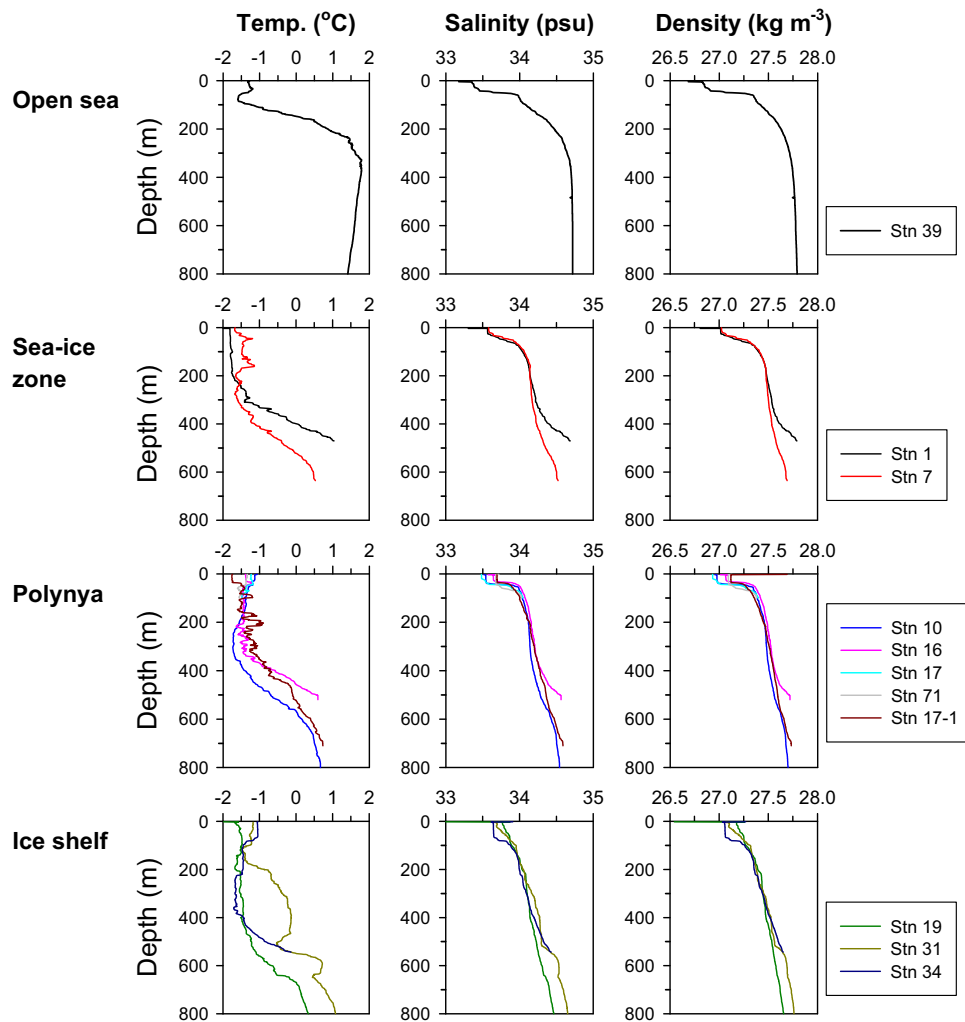


Fig. 2. Vertical profiles of temperature, salinity and density during a late phytoplankton bloom in February in the Amundsen Sea Polynya (ASP). Stn 17-1 denotes that the sampling was conducted at Stn 17 after the bloom in March.

2–4 °C in a refrigerator (Stedmon and Markager, 2001). The absorbance of the samples was measured on board using a double-beam Shimadzu UV-1800 spectrophotometer with a 10-cm quartz cell in the spectral range 350–900 nm. A quartz cell filled with the pre-filtered Milli-Q water was used as the reference for all samples. The absorbance at 375 nm relative to distilled water was measured, and then the absorption coefficient at 375 nm ($CDOM_{(375)} m^{-1}$) was determined (Kowalczyk et al., 2005).

2.2. Microbiological parameters

Samples for enumerating the BA were preserved with glutaraldehyde at a final concentration of 1% and stored in a freezer at -20 °C (Hyun and Yang, 2003). The BA was measured using the DAPI-staining method (Porter and Feig, 1980). More than 20 microscopic fields were examined using an epifluorescence microscope (Nikon, Eclipse 80i) equipped with a mercury lamp (HB-10101 AF), an ultraviolet (UV) excitation filter, and a BA 420 barrier filter.

Heterotrophic BP was estimated from the rate of 3H -thymidine (3H -TdR) incorporation (Fuhrman and Azam, 1980, 1982). Duplicate 20-ml water samples were incubated in the dark with 3H -TdR (final concentration, 10 nM thymidine, Moravsek, MT-6034) at *in situ* water temperature (-2 to -1 °C) for 30 min in disposable plastic centrifuge tubes. At the end of incubation, the samples were collected by vacuum filtration onto 0.2- μm cellulose nitrate membrane filters (MFS). Cold trichloroacetic acid (TCA) insoluble macromolecules

were precipitated using ice-cold TCA (final concentration, 5%) solutions for 15 min, and then rinsed three times with ice-cold 80% ethanol. The filters were placed in scintillation vials. In the lab, after adding 10 ml of scintillation cocktail (Lumagel Safe, Lumac-LSC), the activity of the cold TCA insoluble macromolecules was determined using a liquid scintillation counter (LKB, Rack Beta II). Control samples were treated with 5% TCA before the addition of 3H -TdR. The radioactivity that accumulated in the cold TCA insoluble after the 30 min incubation at the sea-ice zone (average, 2540 dpm), polynya (average, 5513 dpm), ice-shelf (average, 2859 dpm) and open sea site (average, 744 dpm) was higher than the average radioactivity of the killed control by a factor of 5.5, 12.0, 6.2, and 1.6, respectively.

To determine the abundance of heterotrophic nanoflagellates (HNF) that have been identified as potentially important grazers of heterotrophic bacteria in the marine ecosystem (Becquevort et al., 2000; Calbet et al., 2001), 50–100-ml water samples were preserved with glutaraldehyde (1% final concentration), and then stored at 4 °C before staining and filtration. Aliquots of the preserved samples were stained with proflavin (0.33%) for 1 h before filtration, and then filtered onto black 0.45- μm Nucleopore filters. During filtration, the samples were drawn down until 5 mL remained in the filtration funnel. Concentrated DAPI (50 $\mu g mL^{-1}$ final concentration) was then added and allowed to sit briefly (5 s) before the remaining sample was filtered (Taylor et al., 2011). Filters were mounted onto glass slides with immersion oil and cover slips. At least 50 fields per sample were counted with an

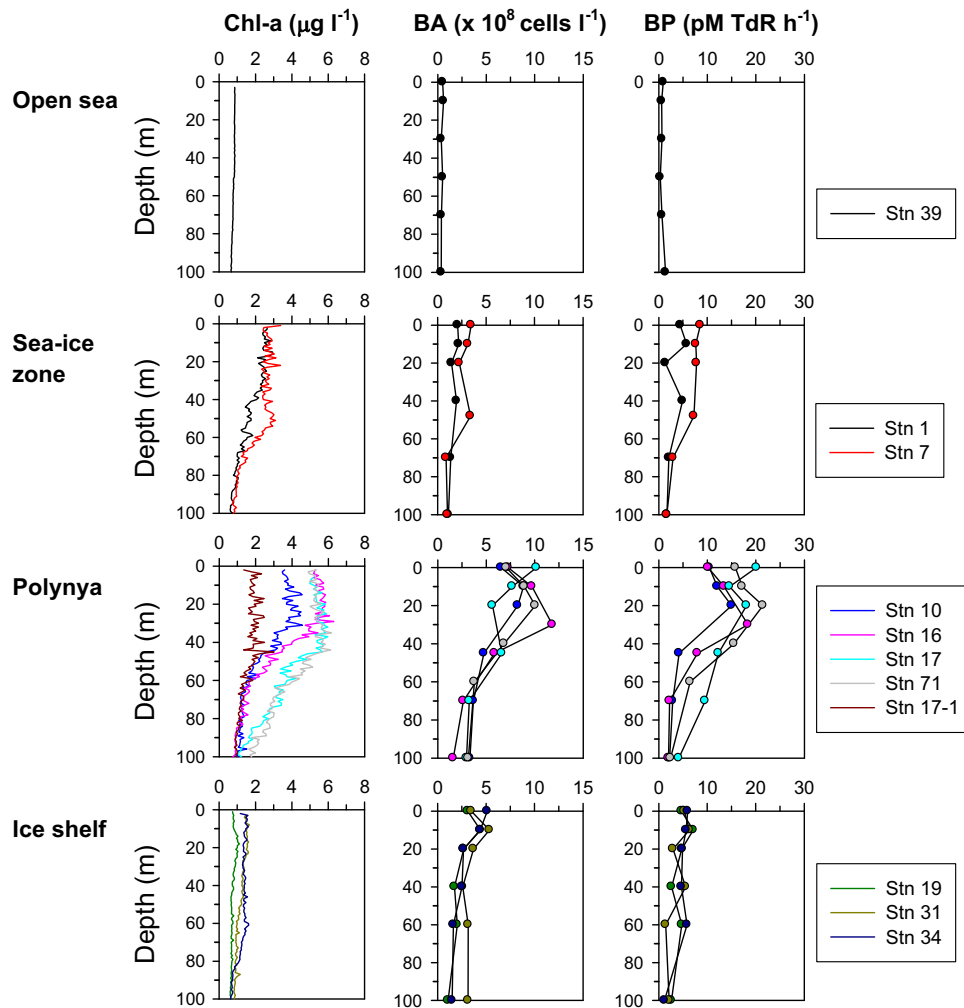


Fig. 3. Vertical profiles of chlorophyll *a* (Chl *a*), bacterial abundance (BA), and bacterial production (BP) during a late phytoplankton bloom in February in the ASP. Stn 17-1 denotes that the sampling was conducted at Stn 17 after the bloom in March.

epifluorescence microscope (Olympus BX 51) at magnifications of 200–640 \times using a blue light excitation filter set for chlorophyll autofluorescence and a UV light excitation filter set for cells stained with DAPI. Autotrophic organisms were distinguished from heterotrophs by the presence of chlorophyll, which was visualized as red fluorescence under blue light illumination.

2.3. Data analysis and conversion factors

Vertical temperature and salinity profiles from the CTD were used to estimate the mixed layer depth (MLD). The MLD was defined as the depth at which the density change exceeded 0.05 kg m^{-3} relative to the density at 10 m (Brainerd and Gregg, 1995). The euphotic depth was defined as the depth at which the irradiance became 1% of its value just under the surface of the water. The phytoplankton C biomass (Chl-C) was converted using a C to Chl *a* ratio (C:Chl *a*) of 50 that was adopted in the Ross Sea when the annual *Phaeocystis* bloom was declining in late summer (January–February) (Ducklow et al., 2000). The C:Chl *a* ratio estimated in the Ross Sea was highly variable from as low as 25 in late spring to 1150 in autumn according to the photo-physiological status of *Phaeocystis* (Smith et al., 2000).

Bacterial carbon biomass (BCB) was estimated using a conversion factor of 10 fg C per cell (Fukuda et al., 1998). To convert thymidine incorporation rates to bacterial cell production, a conversion factor of 8.6×10^{17} cells produced per mol of thymidine incorporated into the cold TCA insoluble material was used, as previously

determined in the Ross Sea (Ducklow et al., 1999). Water column inventories of nitrate, Chl *a*, BA and BP were obtained from the integration of volume-based values at depths down to the surface mixed layer. Total bacterial community growth rates, i.e., biomass turnover rates, were estimated by dividing the mixed-layer depth integrated bacterial production by the integrated bacterial biomass (Kirchman et al., 2009). Primary production for calculating the BP: PP ratio was adopted from Kim et al. (2014a).

3. Results

3.1. Hydrography

In the summer, three major water masses characterize the physical properties of the surface waters of the coastal Southern Ocean (Clarke et al., 2012): (1) fresher and warmer Antarctic Surface Water (AASW) (between depths of 0–50 m at Stn 39); (2) winter water (WW) that is saltier, near freezing, and was formed in the previous winter; and (3) warm CDW flowing into the Amundsen Sea along the bottom of the continental shelf (below a depth of 300 m at Stn 39). The WW is capped by the warmer and fresher AASW, resulting in a subsurface temperature minimum between depths of 50–100 m as seen at Stn 39 (Fig. 2). As it was defined in the Eastern Amundsen Sea (Jacobs et al., 2011), the warm and saline CDW that intrudes onto the continental shelf

Table 1
Oceanographic parameters in the surface water column under different water regimes of the Amundsen Sea, February 10–March 09, 2012.

Oceanographic setting		Stn	Sea-ice coverage (%)	Sampling Date	UTC	Latitude (°S)	Longitude (°W)	Water depth (m)	Euphotic depth (m)	Mixed depth (m)	Temp (°C)	Sal. (psu)	NO ₃ ⁻ -N (μM)	PO ₄ ³⁻ -P (μM)	Chl <i>a</i> (μg L ⁻¹)
Outer shelf	Sea ice zone	1	85.3	10-Feb.	10:18	71.661	116.778	473	27.9	34	-1.81	33.13	21.71	1.703	2.65
		7	46.6	11-Feb.	03:32	72.846	116.503	638	22.8	33	-1.66	33.58	20.54	1.670	3.39
Polynya	Center	10	0	12-Feb.	09:49	73.250	114.998	825	14.8	41	-1.07	34.01	11.33	1.118	3.60
		16	0	14-Feb.	11:00	73.499	113.000	525	18.1	32	-1.40	33.16	14.18	1.312	5.28
		17	0	14-Feb.	18:37	73.500	114.003	711	17.6	38	-1.23	33.48	9.172	0.915	5.16
	Ice shelf	71	0.4	16-Feb.	02:34	73.821	113.067	783	14.8	58	-1.33	33.72	11.84	1.203	5.36
		19	0	16-Feb.	11:40	74.202	112.511	1064	41.8	49	-1.66	33.14	23.88	1.836	0.74
Open sea		31	0	24-Feb.	11:12	75.087	101.759	947	33.1	40	-1.19	33.55	17.78	1.145	1.47
		34	0	25-Feb.	04:28	74.647	101.533	541	26.3	75	-1.04	33.91	16.43	1.330	1.17
		39	0	09-Mar.	06:18	71.581	133.988	3965	15.5	32	-1.29	34.69	24.75	1.837	0.86

Table 2
Depth-integrated (down to the mixed-layer depth unless otherwise indicated) phytoplankton carbon biomass (Chl-C), bacterial carbon biomass (BCB), and abundance of heterotrophic nanoflagellates (HNF), and rates of bacterial production (BP) and bacterial biomass turnover. PP, primary production.

Oceanographic setting		Stn	Chl-C ^a (mmol C m ⁻²)	BCB ^b (mmol C m ⁻²)	BP ^c (mmol C m ⁻² d ⁻¹)		Bacterial turnover rate (d ⁻¹)	BCB /Chl-C (%)	BP _{mld} /PP ^d (%)	BP _{eup} /PP ^d (%)	HNF (× 10 ⁹ cells m ⁻²)
					BP _{mld}	BP _{eup}					
Outer shelf	Sea ice zone	1	342	4.59	1.90	1.52	0.41	1.34	9.3	7.5	25.6
		7	360	7.39	4.47	3.40	0.60	0.61	32.2	24.5	47.7
		Mean (± 1 SD)	351 (13)	5.99 (1.98)	3.18 (1.82)	2.46 (1.33)	0.51 (0.14)	0.98 (0.52)	20.7 (16.2)	16.0 (12.0)	36.7 (15.7)
Polynya	Center	10	630	25.52	8.10	3.49	0.32	4.05	28.4	12.2	107
		16	716	27.00	8.14	4.98	0.30	3.77	25.5	15.6	103
		17	755	20.57	9.84	4.86	0.48	2.73	80.7	39.8	138
		71	1256	36.89	17.33	5.06	0.47	2.94	-	-	240
		Mean (± 1 SD)	839 (283)	27.50 (6.84)	10.85 (4.39)	4.60 (0.74)	0.39 (0.09)	3.37 (0.64)	44.9 (31.0)	22.6 (15.1)	147 (63.9)
Ice shelf		19	170	11.09	4.96	4.23	0.45	6.53	5.1	4.3	50.3
		31	234	12.71	4.28	3.69	0.34	5.43	20.9	18.0	47.8
		34	430	15.69	7.09	3.76	0.45	3.65	-	-	80.5
		Mean (± 1 SD)	278 (135)	13.16 (2.33)	5.44 (1.46)	3.89 (0.29)	0.41 (0.06)	5.20 (1.45)	13.0 (11.2)	11.2 (9.7)	59.5 (18.2)
Open sea		39	107	1.33	0.36	0.19	0.267	1.25	11.8	13.5	

^a Carbon biomass of Chl-*a* was calculated using C:Chl-*a* of 50 that was estimated during bloom in the Ross Sea (Smith et al., 2000).

^b Bacterial carbon biomass was calculated from 10 fg C per cell (Fukuda et al., 1998).

^c Bacterial C production was calculated using conversion factor of 8.67 × 10¹⁷ cells produced per mol TdR (Ducklow et al., 1999) and 10 fg C per cell (Fukuda et al., 1998).

^d Data from Kim et al. (2014).

was observed at depths > 300 m, the salinities > 34.6 psu, and the temperature > 1.5 °C at Stn 39. In contrast, the AASW that is colder than the CDW is distributed in the surface layer over the shelf region (outer shelf-polynya-ice shelf), which is refreshed as the ice melts in the summer (Klinck, 1998). In addition, as the warm CDW is introduced onto the continental shelf, it mixes with the fresh, cold AASW to form Modified Circumpolar Deep Water (MCDW). The MCDW between 100 and 300 m at Stn 39 enters the shallow shelf along deep troughs (Nitsche et al., 2007).

3.2. Physico-chemical environments

Within a water column at a depth of 100 m, where our microbiological analysis was conducted, the water temperature ranged from -1.81 to -1.04 °C, and the salinity was 33.13 to 34.01 psu (Table 1). The lowest surface water temperature was in the sea-ice zone (Stn 1), where the ice cover on the surface water was over 85%. At the open sea site (Stn 39), a strong density gradient appeared at a depth of 50 m. The water temperature between depths of 100–200 m indicated that the CDW mixed with cold AASW at these depths to form MCDW (Fig. 2). The vertical profiles of water temperature, salinity, and density indicated that the salinity gradient resulting from melting ice was the major factor determining the water column density in the surface

water column (Fig. 2). The most pronounced physical feature associated with the spatial distribution of phytoplankton was the strong pycnocline that resulted from the salinity gradient at depths of 30–50 m in the polynya and marginal ice zone in the outer shelf, whereas relatively few physical variations were observed at the ice shelf site. The high temperature and salinity at Stns 31 and 34 (Fig. 2) indicated that an upwelling of warm MCDW occurred at the PIG (Jacobs et al., 2011) during the sampling. In March, the surface temperature at the polynya (Stn 17-1 in Fig. 2) dropped to -1.75 °C.

Both nitrate and phosphate were abundant in the surface water column (Table 1). In near surface water, the nitrate and phosphate concentrations were low in the center of the polynya (11.63 ± 2.06 μM N; 1.14 ± 0.17 μM P) where the highest Chl *a* concentration was observed, whereas higher concentrations were observed at the ice shelf (19.36 ± 3.97 μM N; 1.44 ± 0.36 μM P).

3.3. Microbiological parameters

3.3.1. Phytoplankton biomass

Microscope observations revealed that colonial *P. antarctica* dominated the phytoplankton bloom in the central polynya. Chl *a* concentrations within the surface mixed layer were higher at the polynya stations, ranging from 2.93 to 6.30 μg L⁻¹ (Fig. 3), than at

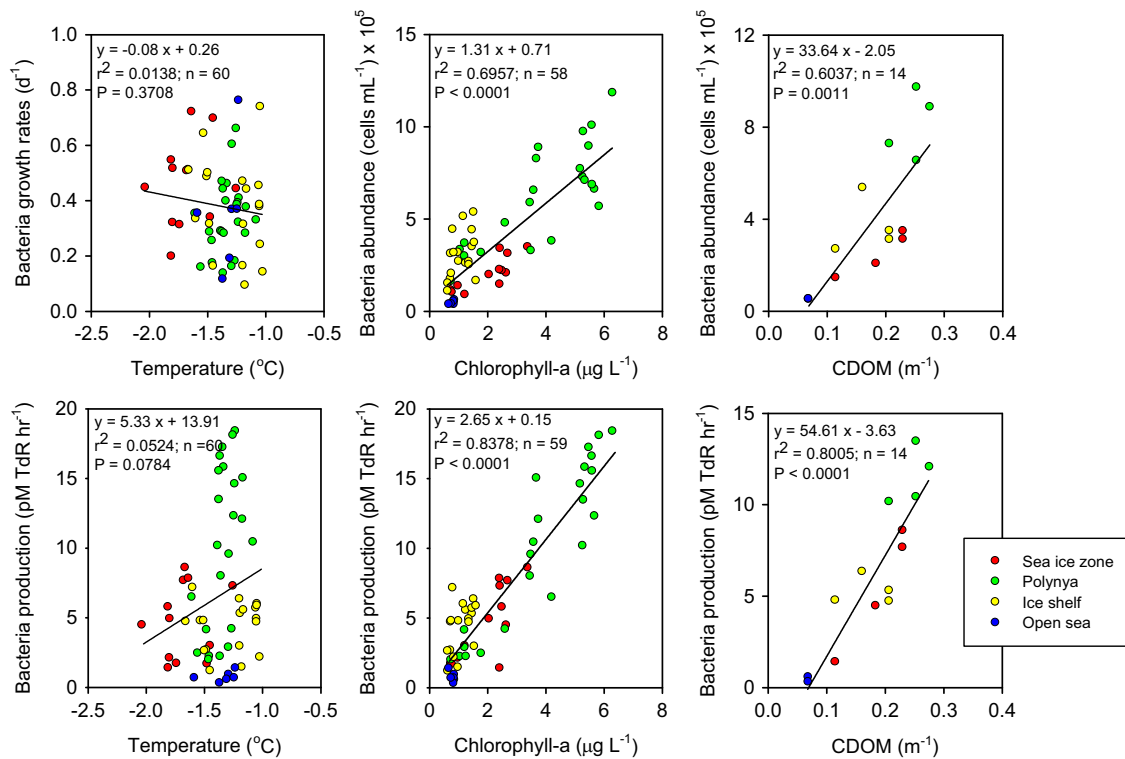


Fig. 4. Relationships between bacterial parameters, and physico-chemical and biological parameters.

the outer shelf ($2.26\text{--}3.39\ \mu\text{g L}^{-1}$), ice shelf ($0.65\text{--}1.67\ \mu\text{g L}^{-1}$) and open sea ($0.85\text{--}0.88\ \mu\text{g L}^{-1}$) sites. There was a uniform vertical distribution of Chl *a* in the polynya and the outer shelf within the surface mixed layer, but the concentration then decreased below the mixed-layer depth. On the other hand, the vertical distribution was homogenous at the open sea and ice shelf sites (Fig. 3). Depth integrated phytoplankton C biomass (Chl-C) at the polynya ($839 \pm 232\ \text{mmol C m}^{-2}$) was higher by factors of 2.4, 3.1, and 7.8 than that at the outer shelf ($351 \pm 13\ \text{mmol C m}^{-2}$), ice-shelf ($278 \pm 136\ \text{mmol C m}^{-2}$), and open sea ($107\ \text{mmol C m}^{-2}$) sites, respectively (Table 2).

3.3.2. Abundance of bacteria and heterotrophic nanoflagellates

The BA in the mixed layer was highest at the polynya, (average, $7.88 \times 10^5\ \text{cells mL}^{-1}$; $4.77\text{--}11.83 \times 10^5\ \text{cells mL}^{-1}$) compared to the outer shelf (average, $2.48 \times 10^5\ \text{cells mL}^{-1}$; $1.44\text{--}3.47 \times 10^5\ \text{cells mL}^{-1}$), ice shelf (average, $3.35 \times 10^5\ \text{cells mL}^{-1}$; $1.64\text{--}5.36 \times 10^5\ \text{cells mL}^{-1}$), and open sea (average, $0.50 \times 10^5\ \text{cells mL}^{-1}$; $0.37\text{--}0.60 \times 10^5\ \text{cells mL}^{-1}$) sites (Fig. 3). The maximum BA observed at the polynya was $1.18 \times 10^6\ \text{cells mL}^{-1}$ at a depth of 30 m at Stn 16. Depth integrated BCB at the polynya ($27.5 \pm 6.8\ \text{mmol C m}^{-2}$) was higher than at the outer shelf ($6.0 \pm 2.0\ \text{mmol C m}^{-2}$), ice-shelf ($13.2 \pm 2.3\ \text{mmol C m}^{-2}$) and open sea ($1.4\ \text{mmol C m}^{-2}$) sites by factors of 4.5, 2.1, and 20, respectively (Table 2). The depth-integrated HNF abundance at the polynya ($146 \pm 64 \times 10^9\ \text{cells m}^{-2}$) was higher than at the outer shelf ($37 \pm 15 \times 10^9\ \text{cells m}^{-2}$), ice shelf ($60 \pm 18 \times 10^9\ \text{cells m}^{-2}$), and offshore ($13.5 \times 10^9\ \text{cells m}^{-2}$) sites by factors of 4, 2.5, and 11, respectively (Table 2).

3.3.3. Bacterial production

The BP was highest at the polynya (average, $10.8\ \text{pM TdR h}^{-1}$; $2.2\text{--}21.5\ \text{pM TdR h}^{-1}$) compared to the outer shelf (average, $4.7\ \text{pM TdR h}^{-1}$; $1.4\text{--}8.6\ \text{pM TdR h}^{-1}$), ice shelf (average, $5.9\ \text{pM TdR h}^{-1}$; $1.2\text{--}12.2\ \text{pM TdR h}^{-1}$) and open sea (average, $0.7\ \text{pM TdR h}^{-1}$; $0.3\text{--}1.4\ \text{pM TdR h}^{-1}$) sites (Fig. 3). The maximum BP was $21.5\ \text{pM TdR h}^{-1}$ at a depth of 20 m at Stn 71. Depth-integrated BP at the polynya

($10.9 \pm 4.4\ \text{mmol C m}^{-2}\ \text{d}^{-1}$) was higher by factors of 3.4, 2.0, and 27.3 compared to the outer shelf ($3.2 \pm 1.8\ \text{mmol C m}^{-2}\ \text{d}^{-1}$), ice-shelf ($5.5 \pm 1.5\ \text{mmol C m}^{-2}\ \text{d}^{-1}$) and open sea ($0.4\ \text{mmol C m}^{-2}\ \text{d}^{-1}$) sites, respectively (Table 2).

3.4. Relationships with temperature, phytoplankton, CDOM, and HNF

The BA and BP data for all sampling sites were pooled, and correlations between bacterial parameters and physico-chemical parameters were determined (Fig. 4). The correlations between temperature and bacterial growth rates ($r^2=0.083$, $P=0.3708$, $n=60$) and between temperature and BP ($r^2=0.0524$, $P=0.0784$, $n=60$) were not significant within the narrow temperature ranges we observed (Fig. 4). Significant positive correlations were obtained between the spatial distribution of Chl *a* and BA ($r^2=0.6957$, $P<0.0001$, $n=58$), and between Chl *a* and BP ($r^2=0.8378$, $P<0.0001$, $n=59$) (Fig. 4). The average BCB accounted for less than 5% of phytoplankton biomass, and BP amounted to 17% of PP on average (Table 2). The highest BP:PP ratio of ca. 0.4 at Stn 17 was due to the unexpectedly low PP at the center of the polynya (Kim et al., 2014a). If this abnormally low PP value was excluded, BP accounted for 13% of the PP on average within the euphotic depth. The absorption coefficients of $\text{CDOM}_{(375)}$ measured in the surface water column during the late bloom ranged from 0.0690 to $0.2764\ \text{m}^{-1}$, and were generally higher at the center of the polynya, where the average value was $0.2476\ \text{m}^{-1}$ (Fig. 4). The $\text{CDOM}_{(375)}$ concentration was lowest at Stn 1 ($0.1152\text{--}0.1842\ \text{m}^{-1}$) in the sea-ice zone where the extent of ice cover was high (85.3%, Table 1). The CDOM concentrations displayed a significant positive correlation with BA ($r^2=0.6037$, $P<0.0011$, $n=14$) and BP ($r^2=0.8005$, $P<0.0001$, $n=14$) (Fig. 4).

The average BCB accounted for less than 5% of phytoplankton biomass, and BP amounted to 17% of PP on average (Table 2). The highest BP:PP ratio of ca. 0.4 at Stn 17 was due to the unexpectedly low PP at the center of the polynya (Kim et al., 2014a). If this abnormally low PP value was excluded, BP accounted for 13% of

the PP on average within the euphotic depth. The absorption coefficients of $CDOM_{(375)}$ measured in the surface water column during the late bloom ranged from 0.0690 to 0.2764 m^{-1} , and were generally higher at the center of the polynya, where the average value was 0.2476 m^{-1} (Fig. 4). The $CDOM_{(375)}$ concentration was lowest at Stn 1 (0.1152–0.1842 m^{-1}) in the sea-ice zone where the extent of ice cover was high (85.3%, Table 1). The $CDOM$ concentrations displayed a significant positive correlation with BA ($r^2=0.6037$, $P < 0.0011$, $n=14$) and BP ($r^2=0.8005$, $P < 0.0001$, $n=14$) (Fig. 4).

To evaluate the prey–predator relationship, we plotted the BA against the HNF abundance (Fig. 5). The average bacteria:HNF ratios were 125 (open sea site), 236 (center of polynya), 280 (ice shelf), and 354 (outer shelf), with an overall average of 260. The ratio was fairly constant at most sites, but was highly variable (136–1340) at the ice-covered outer shelf sites (Stns 1 and 7). Overall, the HNF abundance was significantly correlated with the spatial distribution of BA ($r^2=0.7788$, $P < 0.0001$, $n=60$) (Fig. 5).

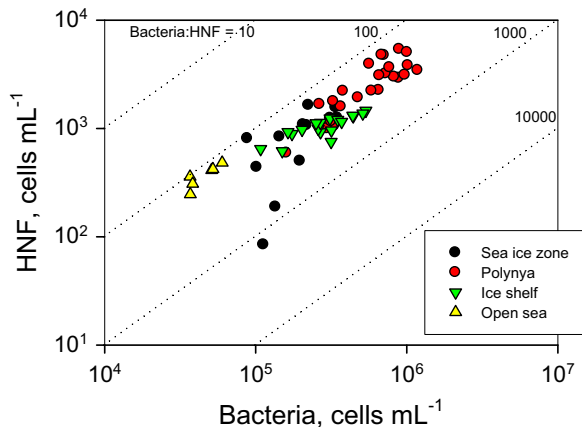


Fig. 5. Relationship between the abundance of bacteria and heterotrophic nanoflagellates (HNF).

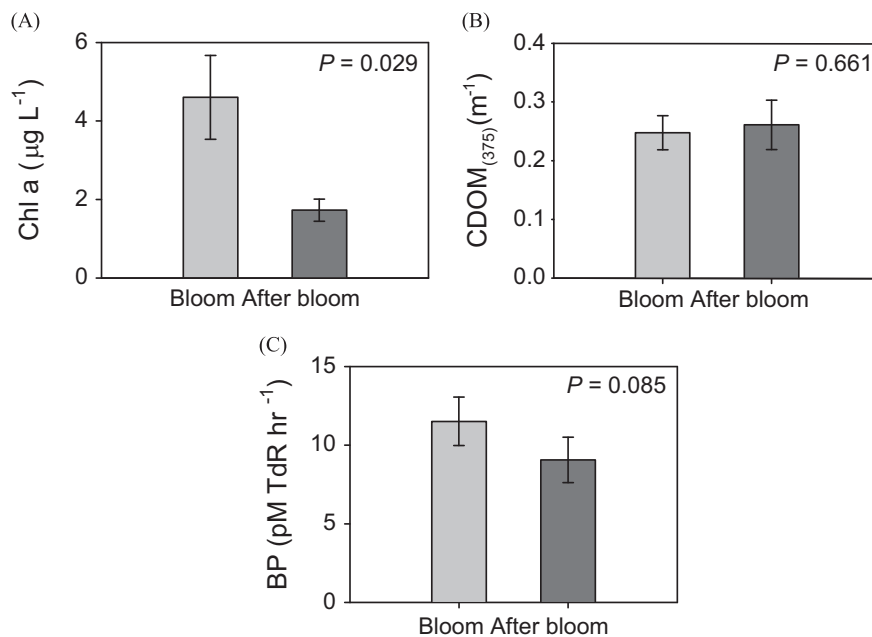


Fig. 6. Concentrations of chlorophyll-*a* (Chl *a*) and chromophoric dissolved organic matter ($CDOM_{(375)}$) and bacterial production (BP) at Stn 17 during the late bloom period and after the bloom. Average numbers were calculated from 3 to 6 different depths within 20 m depth, and *t*-tests were performed to compare the differences between each parameter.

4. Discussion

4.1. Spatial distribution of Chl *a*, BA, and BP

The distribution of Chl *a* displayed large spatial variation, with the highest values at the polynya sites (Fig. 3). Higher Chl *a* concentrations at the center of the polynya were associated with the relatively strong stratification formed by the melting of sea-ice (Table 2, Fig. 2). Yager et al. (2012) reported that in early summer (December–January) the high phytoplankton biomass in the fresher and warmer water reflected the influence of melting sea-ice and the upwelling of glacier-derived melt water, which resulted in stratification of the water column, enhanced solar radiation, and the addition of Fe or other micronutrients to the upper mixed layer. The relatively low Chl *a* concentration at Stns 31 and 34 near the PIG was associated with the well-mixed water column resulting from the upwelling of warm MCDW (Jacobs et al., 2011). Similarly, low Chl *a* concentrations were observed at Stn 19 near the Dotson Ice Shelf, where the surface water column was also well mixed.

The BA and BP in the ASP displayed large spatial variations in accordance with the distribution of Chl *a* (Fig. 4), and were highest at the center of the polynya (Fig. 2, Table 2). The BA ($1.44\text{--}11.83 \times 10^5$ cells mL^{-1}) and BP ($8.1\text{--}17.3$ $mmol\ C\ m^{-2}\ d^{-1}$) in this study (February) were higher than the corresponding values in early summer (BA, $1.2\text{--}7.5 \times 10^5$ cells mL^{-1} ; BP, $0.02\text{--}0.23$ $mmol\ C\ m^{-2}\ d^{-1}$) (Yager et al., 2012). Because the phytoplankton parameters ($PP=2.2$ $g\ C\ m^{-2}\ d^{-1}$; Chl *a*=395 $mg\ m^{-2}$) were higher in January (Lee et al., 2012) than in February ($PP=0.25$ $g\ C\ m^{-2}\ d^{-1}$; Chl *a*=143 $mg\ m^{-2}$) (Kim et al., 2014a), our results of a higher BA and BP in late summer (February) than in early summer (January) indicated a time lag between the bacterial and *Phaeocystis* blooms. A similar time lag has been reported in the Ross Sea Polynya (ca. 30 days, Ducklow et al., 2001), Prydz Bay and the Weddell Sea (15–30 days, Billen and Becquevort (1991)).

4.2. Control of BP

In the Amundsen Sea, the rapid melting of the glaciers and ice-shelves resulting from the intrusion of CDW and the upwelling of

warm MCDW (Jacobs et al., 1996; Jenkins et al., 2010) may release a substantial amount of Fe into surface waters to support phytoplankton blooms (Gerringa et al., 2012; Thuróczy et al., 2012) and presumably bacterial growth. Given that Fe is available from melting ice and inorganic nutrients are abundant (Table 1) in the Southern Ocean, temperature and DOC are likely the two main controls that limit bacterial growth in the polar seas (Kirchman et al., 2009; Pomeroy and Deibel, 1986). Kirchman et al. (2009) found a positive relationship between temperature and bacterial growth in the oceans, including polar seas. However, based on the unexpectedly high Q10 (> 100) at temperatures below 0 °C, they concluded that the positive relationship between temperature and bacterial parameters was largely determined by other factors that co-vary with temperature. Indeed, previous studies in the Ross Sea also found no direct effect of temperature on BP (Carlson et al., 1998; Ducklow et al., 2001). In this study, the relationship between bacterial growth and bacterial production was not significantly correlated with temperature, even below 0 °C (Fig. 4).

In contrast to temperature, BP was significantly correlated with phytoplankton biomass ($r^2=0.8378$, $P<0.0001$) and CDOM₍₃₇₅₎ ($r^2=0.8005$, $P<0.0001$) (Fig. 4). These relationships suggest that DOC, which originates from phytoplankton, significantly promotes the maintenance of the high BP during the late *Phaeocystis* bloom. The DOC produced from the phytoplankton is available for stimulating bacterial growth through a variety of mechanisms such as direct extracellular release, sloppy feeding on phytoplankton by zooplankton, viral lysis, and solubilization by heterotrophic bacteria attached to particles (see Nagata, 2008). A coupling between bacteria and phytoplankton has been well established in the Southern Ocean (Cota et al., 1990; Ducklow et al., 1999; Lochte et al., 1997; Morán et al., 2001).

To further demonstrate the dependence of BP on DOC, we revisited the center of the polynya in March (i.e., Stn 17-1 that is denoted as Stn 17 in February, Figs. 2 and 3). The Chl *a* concentrations significantly decreased after the bloom declined (i.e., from $4.6 \pm 1.1 \mu\text{g L}^{-1}$ during the late bloom to $1.7 \pm 0.3 \mu\text{g L}^{-1}$ after the bloom, $P=0.029$, Fig. 6A). Despite the significant decrease in phytoplankton biomass, the mean CDOM₍₃₇₅₎ concentration after the bloom ($0.25 \pm 0.03 \text{ m}^{-1}$) was not significantly different from the CDOM₍₃₇₅₎ measured during the bloom ($0.26 \pm 0.04 \text{ m}^{-1}$, $P=0.661$, Fig. 6B). Similarly, the BP during the bloom ($11.5 \pm 1.5 \text{ pM TdR h}^{-1}$) did not significantly decrease after the bloom ($9.1 \pm 1.4 \text{ pM TdR h}^{-1}$) ($P=0.085$, Fig. 6C). Therefore, the high BP and CDOM₍₃₇₅₎ that persisted after the *Phaeocystis* bloom further supported that BP was sustained by the DOC that remained in the system after the bloom. It is well-known that DOC accumulation occurs in the water column during and after the bloom or productive period. For example, Billen and Fontigny (1987) observed a rapid increase in DOC during a spring bloom of *Phaeocystis pouchetii*, and high concentrations (almost 5 mg CL^{-1}) remained after the *Phaeocystis* bloom on the Belgian coast. Carlson et al. (2000) also reported that both DOC and POC accumulated as a spring bloom of *P. antarctica* progressed, with maximum concentrations of 46–55 μM DOC and $> 100 \mu\text{M}$ POC in the top 50 m during late summer (February). They reported that the DOC produced during the *Phaeocystis* bloom was relatively labile and turned over within 6 months, reaching a background level in late winter. Similarly, Kirchman et al. (2001) reported that DOC (mostly polysaccharides) increased at least threefold during a *Phaeocystis* bloom in the Ross Sea, and argued that the accumulation of dissolved polysaccharides and other semi-labile DOCs have the potential to support high BP even after the bloom.

In the present study, CDOM₍₃₇₅₎ was used as a proxy of DOM to stimulate BP after the bloom (Fig. 6). CDOM is generally known to be produced by bacteria using non-fluorescent organic matter derived from phytoplankton (Rochelle-Newall and Fisher, 2002). CDOM may also be generated directly through extracellular release by prokaryotes, and excretion by zooplankton and Antarctic krill (Nelson et al., 2004;

Steinberg et al., 2004; Urban-Rich et al., 2006; Ortega-Retuerta et al., 2009). The photolysis of CDOM also results in the release of low-molecular-weight compounds, which can be an important labile substrate for microbial communities (Morán and Zepp, 1997). Obernosterer et al. (2001) reported that in the central Crozet Basin in the Southern Ocean, DOM with initially low bioavailability could be photochemically transformed to compounds with higher bioavailability.

4.3. Control of BA

Despite the general consensus that bacterial production is coupled with phytoplankton, a few studies reported that protozoan grazing could induce a weak coupling between bacteria and phytoplankton (Bird and Karl, 1999; Duarte et al., 2005). During a spring bloom in the Gerlache Strait, Bird and Karl (1999) reported that the bacterial biomass was $< 2\%$ of the total plankton biomass, and BP was $\sim 3\%$ of the corresponding PP, which implied that the microbial loop was uncoupled from primary producers during the spring bloom period. Based on prey–predator plotting that revealed a bacteria:HNF ratio of 85, they speculated that protozoan grazing on bacteria was largely responsible for the uncoupling.

In this study, the bacteria:HNF ratio was 260 on average (Fig. 5), which was lower than the range (400–1000) reported in most marine environments (Sanders et al., 1992) including the Ross Sea Polynya (800) where the bacteria:HNF ratio approached 10,000 in some samples (Ducklow and Yager, 2006). In addition, the mean BA in the mixed layer of the ASP in the present study (February, $7.88 \times 10^5 \text{ cells mL}^{-1}$) was lower than that observed in the same season in the Ross Sea Polynya ($11.5 \times 10^5 \text{ cells mL}^{-1}$, Ducklow et al., 2001), although the BP was higher in the ASP than in the Ross Sea Polynya. In addition to the low bacteria:HNF ratio, a direct grazing experiment conducted along with this study revealed that bacterivory removed average 93% (51–144%) of BP, and consumed 27% (12–53%) of bacterial standing stock in the ASP (Yang EJ, unpublished data). These results strongly suggest that heterotrophic protozoa effectively control the bacterial biomass during the late bloom in the ASP.

The large number of HNF grazing on bacteria (i.e., low bacteria:HNF ratio) may reflect the existence of an intermediate trophic level between krill and bacterivores in the Antarctic waters (Ducklow and Yager, 2006). The grazing control of mesozooplankton on heterotrophic bacteria via a trophic cascade (i.e., mesozooplankton – microprotozooplankton – nanoprotozooplankton – bacteria) in coastal marine ecosystems has been well documented. For example, based on a mesocosm experiment, Zöllner et al. (2009) demonstrated that high copepod grazing on microzooplankton (ciliates) suppressed BA by enhancing the amount of HNF grazing on bacteria. In the Southern Ocean, Yang et al. (2012) also demonstrated an inverse relationship between microprotozoa and heterotrophic nanoprotozoa (i.e., bacterivores), along the Weddell Sea–Scotia Sea Transect.

Investigations on the zooplankton composition and distribution conducted along with our study in February (Lee et al., 2013) and that conducted earlier in January (Wilson et al., 2015) revealed that copepod abundance was low in the ASP, and the mesozooplankton biomass was dominated by the ice krill, *Euphausia crystallorophias* (Lee et al., 2013; La et al., 2015; Wilson et al., 2015). Ko et al. (2015) based on a trophodynamic analysis using fatty acids and stable isotopes, further demonstrated that adult *E. crystallorophias* did not graze on *Phaeocystis*, but rather displayed a carnivorous feeding behavior. Therefore, if the krill effectively suppress the biomass of microzooplankton (Ko et al., 2015) that would otherwise actively graze on the HNF ($< 10 \mu\text{m}$), then the HNF could act as a control on bacteria biomass, resulting in a relatively low bacteria:HNF.

4.4. Significance of the microbial loop during a late bloom

The major components of the microbial loop are the supply of DOM originating from phytoplankton, the uptake of DOM by heterotrophic bacteria, and the consumption of the bacteria by heterotrophic protists (Azam et al., 1983). Therefore, to establish the significance of the microbial loop in the microbial food web process in the ASP, the bacteria should consume a significant portion of primary production via production and/or respiration, and the bacteria should be effectively consumed by bacterivores (see Ducklow and Yager, 2006). In the present study, the average BP:PP ratio of 17% (Table 2) was higher than that reported during the *Phaeocystis* bloom in the Ross Sea (ca. 10%, Kirchman et al., 2009). The BP:PP ratio in the Southern Ocean varies according to the stage of the phytoplankton bloom (Cota et al., 1990; Lochte et al., 1997; Ducklow et al., 2001; Obernosterer et al., 2008; Manganelli et al., 2009). In general, a small proportion of the PP is consumed by BP in the early phase and during the bloom, but the consumption by BP increases during the decline of the bloom. For example, BP accounted for 76% of PP during the austral autumn, but only 14% in the spring (Cota et al., 1990). In the Ross Sea, Ducklow et al. (2001) estimated a BP:PP ratio of 0.04 in October, 0.11 in January, and 0.81 in April, which reflected the variations in BP:PP according to the different stages of the *P. antarctica* bloom. Consequently, in light of the low bacteria:HNF ratio (i.e., intense grazing on bacteria, Fig. 5) in the present study and the fact that both copepod and krill do not significantly consume *Phaeocystis* (Hansen et al., 1993; Haberman et al., 2003; Ko et al., 2015), the high BP:PP ratio suggested that a substantial amount of PP was likely channeled to nano- and microprotzooplankton via the microbial loop, rather than being directly transferred to metazoa via a conventional grazing food web during a late bloom. Based on mixed culture experiments for protozoa and copepod grazing on *Phaeocystis*, Hansen et al. (1993) found that protozoa rather than copepods were responsible for the declining numbers of *Phaeocystis*. In addition, Shields and Smith (2008) demonstrated that microzooplankton (ciliates) consume *Phaeocystis* in the Ross Sea, which also implies that a substantial fraction of *P. antarctica* colonies directly enter the microbial loop before sinking.

Because high bacterial activity may prevent a significant fraction of large phytoplankton from reaching metazoan consumers (Legendre and Fèvre 1995), the microbial loop plays a significant role in determining the efficiency of the export of biogenic carbon. The BP:PP ratio and the export flux are inversely related (Cho et al., 2001), implying that the large bacterial contribution to organic carbon mineralization during the late *Phaeocystis* bloom will diminish the export flux. Indeed, the export flux from the euphotic zone accounted for 30% (14–53%) of PP in the polynya and ice shelf during the late bloom in February (Kim et al., 2014c), whereas approximately 60% of the PP was exported during relatively earlier bloom in January (Yager et al., 2012). Consequently, the high BP:PP ratio reflecting the lower export production in the surface water, together with the active mineralization of organic matter by bacterial respiration within the mesopelagic layer (50–350 m) of the ASP (Ducklow et al., 2015) further implied that the functioning of the biological pump could be weakened during the *Phaeocystis* bloom in the ASP.

Acknowledgments

We thank the captain and crew of the Korean Research Icebreaker, Araon, for their assistance, and Dr. T.W. Kim for providing the site map. We also thank Prof. H.W. Ducklow and two reviewers for their valuable comments that improved the earlier version of

the manuscript. This research was funded by the Korea Polar Research Institute (PP15020).

References

- Alderkamp, A.-C., Mills, M.M., van Dijken, G.L., Laan, P., Thuroczy, C.-E., Gerringa, L., de Baar, H.J.W., Payne, C., Tortell, P., Visser, R.J.W., Buma, A.G.J., Arrigo, K.R., 2012. Iron from melting glaciers fuels phytoplankton blooms in Amundsen Sea (Southern Ocean): phytoplankton characteristics and productivity. *Deep-Sea Res. II* 71–76, 32–48.
- Arrigo, K.R., van Dijken, G.L., 2003. Phytoplankton dynamics within 37 Antarctic coastal polynya systems. *J. Geophys. Res.* 108 (C8), 3271. <http://dx.doi.org/10.1029/2002JC001739>.
- Arrigo, K.R., van Dijken, G., Long, M., 2008. Coastal Southern Ocean: a strong anthropogenic CO₂ sink. *Geophys. Res. Lett.* 35, L21602. <http://dx.doi.org/10.1029/2008GL035624>.
- Arrigo, K.R., Lowry, K.E., van Dijken, G.L., 2012. Annual changes in sea ice and phytoplankton in polynyas of the Amundsen Sea, Antarctica. *Deep-Sea Res. II* 71–76, 5–15.
- Azam, F., Fenchel, T., Field, J.G., Gray, J.S., Meyer-Reil, L.A., Thingstad, F., 1983. The ecological role of water-column microbes in the sea. *Mar. Ecol. Prog. Ser.* 10, 257–263.
- Becquevort, S., Menon, P., Lancelot, C., 2000. Differences of the protozoan biomass and grazing during spring and summer in the Indian sector of the Southern Ocean. *Polar Biol.* 23, 309–310.
- Billen, G., Fontigny, A., 1987. Dynamics of a *Phaeocystis*-dominated spring bloom in Belgian coastal waters. II. Bacterioplankton dynamics. *Mar. Ecol. Prog. Ser.* 37, 249–257.
- Billen, G., Becquevort, S., 1991. Phytoplankton-bacteria relationship in the Antarctic marine ecosystem. *Polar Res.* 10, 245–253.
- Bird, D.F., Karl, D.M., 1999. Uncoupling of bacteria and phytoplankton during the austral spring bloom in Gerlache Strait Antarctic Peninsula. *Aquat. Microb. Ecol.* 19, 13–27.
- Brainger, K.E., Gregg, M.C., 1995. Surface mixed and mixing layer depths. *Deep-Sea Res. I* 42 (9), 1521–1543.
- Calbet, A., Landry, M.R., Nunnery, S., 2001. Bacteria-flagellate interactions in the microbial food web of the oligotrophic subtropical North Pacific. *Aquat. Microb. Ecol.* 23, 283–292.
- Carlson, C.A., Ducklow, H.W., Hansell, D.A., Smith Jr., W.O., 1998. Organic carbon partitioning during spring phytoplankton blooms in the Ross Sea polynya and the Sargasso Sea. *Limnol. Oceanogr.* 43 (3), 375–386.
- Carlson, C.A., Hansell, D.A., Peltzer, E.T., Smith Jr., W.O., 2000. Stocks and dynamics of dissolved and particulate organic matter in the southern Ross Sea, Antarctica. *Deep-Sea Res. II* 47, 3201–3225.
- Carlson, C.A., 2002. Production and removal processes. In: Hansell, D.A., Carlson, C. A. (Eds.), *Biogeochemistry of Marine Dissolved Organic Matter*. Elsevier Academic Press, pp. 91–139.
- Cavaliere, D.J., Parkinson, C.L., Gloersen, P., Zwally, H., 1996. Sea Ice Concentrations from Nimbus-7 SMMR and DMSP SSM/I-SSMIS Passive Microwave Data. 2012. NASA DAAC at the National Snow and Ice Data Center, Boulder, Colorado USA.
- Cho, B.C., Park, M.G., Shim, J.H., Choi, D.H., 2001. Sea-Surface Temperature and f-ratio Explain Large Variability in the Ratio of Bacterial Production to Primary Production in the Yellow Sea. *Mar. Ecol. Prog. Ser.* 216, 31–41.
- Clarke, A., Barnes, D.K.A., Bracegirdle, T.J., Ducklow, H.W., King, J.C., Meredith, M.P., Murphy, E.J., Peck, L.S., 2012. The impact of regional climate change on the marine ecosystem of the western Antarctic Peninsula. In: Rogers, A.D., Johnston, A., Murphy, E.J., Clarke, A. (Eds.), *Antarctic Ecosystems*. Wiley-Blackwell, pp. 93–120.
- Cota, G.F., Kottmeier, S.T., Robinson, D.H., Smith Jr., W.O., Sullivan, C.W., 1990. Bacterioplankton in the marginal ice zone of the Weddell Sea: biomass, production and metabolic activities during austral autumn. *Deep-Sea Res.* 37 (7), 1145–1167.
- del Giorgio, P.A., Cole, J.J., Cimleris, A., 1997. Respiration rates in bacteria exceed phytoplankton production in unproductive aquatic systems. *Nature* 385, 148–151.
- del Giorgio, P.A., Williams, P.J.B., 2005. The global significance of respiration in aquatic ecosystems: from single cells to the biosphere. In: del Giorgio, P.A., Williams, P.J. Le.B. (Eds.), *Respiration in Aquatic Ecosystems*. Oxford University Press, New York, pp. 267–303.
- Delmont, T.O., Hammar, K.M., Ducklow, H.W., Yager, P.L., Post, A.F., 2014. *Phaeocystis antarctica* blooms strongly influence bacterial community structures in the Amundsen Sea polynya. *Front. Microbiol.* 5, 1–13. <http://dx.doi.org/10.3389/fmicb.2014.00646>.
- Duarte, C.M., Agusti, S., Vaqué, D., Agawin, N.S.R., Felipe, J., Casmayor, E.O., Gasol, J. M., 2005. Experimental test of bacteria-phytoplankton coupling in the Southern Ocean. *Limnol. Oceanogr.* 50 (6), 1844–1854.
- Ducklow, H.W., 2000. Bacterial production and biomass in the oceans. In: Kirchman, D.L. (Ed.), *Microbial Ecology of the Oceans*. Wiley-Liss, New York, pp. 85–120.
- Ducklow, H.W., Carlson, C.A., Church, M.J., Kirchman, D.L., Smith, D.C., Steward, G., 2001. The seasonal development of the bacterioplankton bloom in the Ross Sea Antarctica 1994–1997. *Deep-Sea Res. II* 48, 4199–4221.
- Ducklow, H.G., Carlson, C., Smith Jr., W.O., 1999. Bacterial growth in experimental plankton assemblages and seawater cultures from the *Phaeocystis antarctica* bloom in the Ross Sea, Antarctica. *Aquat. Microb. Ecol.* 19, 215–227.

- Ducklow, H.W., Dickson, M.-L., Kirchman, D.L., Steward, G., Orcharado, J., Marra, J., Azam, F., 2000. Constraining bacterial production, conversion efficiency and respiration in the Ross Sea, Antarctica, January–February, 1997. *Deep-Sea Res. II* 47, 3227–3247.
- Ducklow, H.W., Purdie, D.A., Williams, P.J. Le.B., Davies, J.M., 1986. Bacterioplankton: a sink for carbon in a coastal marine plankton community. *Science* 232, 865–867.
- Ducklow, H.W., Wilson, S.E., Post, A.F., Stammerjohn, S.E., Erickson, M., Lee, S., Lowry, K. E., Sherrell, R.M., Yager, P.L., 2015. Particle flux on the continental shelf in the Amundsen Sea Polynya and Western Antarctic Peninsula. *Elem. Sci. Anth.* 3, 000046.
- Ducklow, H.W., Yager, P.L., 2006. Pelagic bacteria in polynyas. In: Smith Jr., W.O., Barber, D. (Eds.), *Polynyas: Windows into Polar Oceans* (Elsevier Oceanography Series), pp. 323–361.
- Fragoso, G.M., Smith Jr., W.O., 2012. Influence of hydrography on phytoplankton distribution in the Amundsen and Ross Seas, Antarctica. *J. Mar. Syst.* 89, 19–29.
- Fuhrman, J.A., Azam, F., 1980. Bacterioplankton secondary production estimates for coastal waters of British Columbia, Antarctica, and California. *Appl. Environ. Microbiol.* 39, 1085–1095.
- Fuhrman, J.A., Azam, F., 1982. Thymidine incorporation as a measure of heterotrophic bacterioplankton production in marine surface waters: evaluation and field results. *Mar. Biol.* 66, 109–122.
- Fukuda, R., Ogawa, H., Nagata, T., Koike, I., 1998. Direct determination of carbon and nitrogen contents of natural bacterial assemblages in marine environments. *Appl. Environ. Microbiol.* 64, 3352–3358.
- Gerringa, L.J.A., Alderkamp, A.-C., Laan, P., Thuróczy, C.-E., deBaar, H.J.W., Mills, M. M., vanDijken, G.L., vanHaren, H., Arrigo, K.R., 2012. Iron from melting glaciers fuels the phytoplankton blooms in Amundsen Sea (Southern Ocean): Iron biogeochemistry. *Deep-Sea Res. II* 71–76, 16–31.
- Hansen, F.C., Reckermann, M., Klein Breteler, W.C.M., Riegman, R., 1993. *Phaeocystis* blooming enhanced by copepod predation on protozoa: evidence from incubation experiments. *Mar. Ecol. Prog. Ser.* 102, 51–57.
- Haberman, K.L., Ross, R.M., Quetin, L.B., 2003. Diet of the Antarctic krill (*Euphausia superba* Dana): II. Selective grazing in mixed phytoplankton assemblage. *J. Exp. Mar. Biol. Ecol.*, 283, pp. 97–113.
- Hyun, J.-H., Yang, E.J., 2003. Freezing seawater for the long-term storage of bacterial cells for microscopic enumeration. *J. Microbiol.* 41, 262–265.
- Jacobs, S.S., Hellmer, H.H., Jenkins, A., 1996. Antarctic ice sheet melting in the southeast Pacific. *Geophys. Res. Lett.* 23 (9), 957–960. <http://dx.doi.org/10.1029/96GL00723>.
- Jacobs, S.S., Jenkins, A., Giulivi, C.F., Dutrieux, P., 2011. Stronger ocean circulation and increased melting under Pine Island Glacier ice shelf. *Nat. Geosci.* 4, 519–523.
- Jenkins, A., Vaughan, D.G., Jacobs, S.S., Hellmer, H.H., Keys, J.R., 1997. Glaciological and oceanographic evidence of high melt rates beneath Pine Island glacier West Antarctica. *J. Glaciol.* 43 (144–121).
- Jenkins, A., Dutrieux, P., Jacobs, S.S., McPhail, S.D., Perrett, J.R., Webb, A.T., White, D., 2010. Observations beneath Pine Island Glacier in west Antarctica and implication for its retreat. *Nat. Geosci.* 3, 468–472.
- Kim, B.K., Joo, H.T., Song, H.J., Yang, E.J., Lee, S.H., Hahn, D., Rhee, T.S., Lee, S.H., 2014a. Large seasonal variation in phytoplankton production in the Amundsen Sea. *Polar Biol.* 38, 319–331. <http://dx.doi.org/10.1007/s00300-014-1588-5>.
- Kim, J.-G., Park, S.-J., Quan, Z.-X., Jung, M.-Y., Cha, I.-T., Kim, S.-J., Kim, K.-H., Yang, E.-J., Kim, Y.-N., Lee, S.-H., Rhee, S.-K., 2014b. Unveiling abundance and distribution of planktonic *Bacteria* and *Archaea* in a polynya in Amundsen Sea, Antarctica. *Environ. Microbiol.* 16; b, pp. 1566–1578.
- Kim, M.S., Chio, M.S., Lee, S.H., Lee, S.H., Rhee, T.S., Hahn, D., 2014c. Estimation of POC export fluxes using $^{234}\text{Th}/^{238}\text{U}$ disequilibria in the Amundsen Sea, Antarctica; preliminary result. *J. Korean Soc. Oceanogr.* 19 (2), 109–124.
- Kirchman, D.L., Meon, M., Ducklow, H.W., Carlson, C.A., Hansell, D.A., Steward, G.F., 2001. Glucose fluxes and concentrations of dissolved combined neutral sugars (polysaccharides) in the Ross Sea and Polar Front Zone, Antarctica. *Deep-Sea Res. II* 48, 4179–4197.
- Kirchman, D.L., 2008. Introduction and overview. In: Kirchman, D.L. (Ed.), *Microbial Ecology of the Oceans*. Wiley-Blackwell, New Jersey, pp. 1–593.
- Kirchman, D.L., Morán, X.A.G., Ducklow, H., 2009. Microbial growth in the polar oceans – role of temperature and potential impact of climate change. *Nat. Rev. Microbiol.* 7, 451–459.
- Klinck, J.M., 1998. Heat and salt changes on the continental shelf in west of the Antarctic Peninsula between January 1993 and January 1994. *J. Geophys. Res. Oceans* 103, 7617–7636.
- Ko, A.-R., Yang, E.J., Kim, M.-S., Ju, S.-J., 2015. Trophodynamics of euphausiids in the Amundsen Sea during the austral summer by fatty acid and stable isotopic signatures. *Deep-Sea Res. II* . <http://dx.doi.org/10.1016/j.dsr2.2015.04.023>.
- Kowalczuk, P., Stoń-Egiert, J., Copper, W.J., Whitehead, R.F., Durako, M.J., 2005. Characterization of chromophoric dissolved organic matter (CDOM) in the Baltic Sea by excitation emission matrix fluorescence spectroscopy. *Mar. Chem.* 96, 273–292.
- La, H.S., Lee, H., Fielding, S., Kang, D., Ha, H.K., Atkinson, A., Park, J., Siegel, V., Lee, S. H., Shin, H.C., 2015. High density of ice krill (*Euphausia crystallorophias*) in the Amundsen sea coastal polynya, Antarctica. *Deep-Sea Res. I* 95, 75–84.
- Lee, D.B., Chio, K.H., Ha, H.K., Yang, E.J., Lee, S.H., Lee, S.H., Shin, H.C., 2013. Mesozooplankton distribution patterns and grazing impacts of copepods and *Euphausia crystallorophias* in the Amundsen Sea, West Antarctica, during austral summer. *Polar Biol.* 36, 1215–1230.
- Lee, S.H., Kim, B.K., Yun, M.S., Joo, H., Yang, E.J., Kim, Y.N., Shin, H.C., Lee, S., 2012. Spatial distribution of phytoplankton productivity in the Amundsen Sea, Antarctica. *Polar Biol.* . <http://dx.doi.org/10.1007/s00300-012-1220-5>
- Legendre, L., Fèvre, J.L., 1995. Microbial food webs and the export of biogenic carbon in oceans. *Aquat. Microb. Ecol.* 9, 69–77.
- Lochte, K., Bjornsen, P.K., Giesenhagen, H., Webers, A., 1997. Bacterial standing stock and production and their relation to phytoplankton in the Southern Ocean. *Deep-Sea Res. II* 44, 321–340.
- Manganelli, M., Malfatti, F., Samo, T.J., Mitchell, B.G., Wang, H., Azam, F., 2009. Major role of microbes in carbon fluxes during austral winter in the Southern Drake Passage. *PLoS One* 4 (9), e6941. <http://dx.doi.org/10.1371/journal.pone.0006941>.
- Miller, L.A., DiTullio, G.R., 2007. Gas fluxes and dynamics in polynyas. In: Smith, W. O., Barber, D.G. (Eds.), *Polynyas: Windows to the World*. Elsevier, Amsterdam, pp. 163–191.
- Montes-Hugo, M.A., Yuan, X., 2012. Climate patterns and phytoplankton dynamics in Antarctic latent heat polynyas. *J. Geophys. Res.* 117, C05031. <http://dx.doi.org/10.1029/2010JC006597>.
- Morán, M.A.G., Zepp, R.G., 1997. Role of photoreactions in the formation of biologically labile compounds from dissolved organic matter. *Limnol. Oceanogr.* 42, 1307–1316.
- Morán, M.A.G., Gasol, J.M., Pedros-Alio, C., Estrada, M., 2001. Dissolved and particulate primary production and bacterial production in offshore Antarctic waters during austral summer: coupled or uncoupled? *Mar. Ecol. Prog. Ser.* 222, 25–39.
- Nagata, T., 2008. Organic matter-bacteria interactions in seawater. In: Kirchman, D. L. (Ed.), *Microbial Ecology of the Oceans*. Wiley, pp. 207–241.
- Nelson, N.B., Carlson, C.A., Steinberg, D.K., 2004. Production of chromophoric dissolved organic matter by Sargasso Sea microbes. *Mar. Chem.* 89, 273–287.
- Nihasi, S., Ohshima, K.I., 2015. Circumpolar mapping of Antarctic coastal polynyas and landfast sea ice: relationship and variability. *J. Clim.* 28, 3650–3670. <http://dx.doi.org/10.1175/JCLI-D-14-00369.1>.
- Nitsche, F., Jabobs, S.S., Larter, R.D., Gohl, K., 2007. Bathymetry of the Amundsen Sea continental shelf: Implications for geology, oceanography, and glaciology. *Geochim. Geophys. Geosyst.* 8, Q10009. <http://dx.doi.org/10.1029/2007GC001694>.
- Obernosterer, I., Sempéré, R., Herndl, G.J., 2001. Ultraviolet radiation induces reversal of the bioavailability of DOM to marine bacterioplankton. *Aquat. Microb. Ecol.* 24, 61–68.
- Obernosterer, I., Christaki, U., Lefèvre, D., Catala, P., Wambeke, F.V., Lebaron, P., 2008. Rapid bacterial mineralization of organic carbon produced during a phytoplankton bloom induced by natural iron fertilization in the Southern Ocean. *Deep-Sea Res. II* 55, 777–789.
- Ortega-Retuerta, E., Frazer, T.K., Duarte, C.M., Ruiz-Halpern, S., Tova-Sánchez, A., Arrieta, J. M., Reche, I., 2009. Biogeneration of chromophoric dissolved organic matter by bacteria and krill in the Southern Ocean. *Limnol. Oceanogr.* 54, 1941–1950.
- Parsons, T.D., Whitney, F.A., Harrison, P.J., 2005. Macronutrient dynamics in an anticyclonic mesoscale eddy in the Gulf of Alaska. *Deep-Sea Res. II* 52, 909–932. <http://dx.doi.org/10.1016/j.dsr2.2005.02.004>.
- Pomeroy, L.R., Deibel, D., 1986. Temperature regulation of bacterial activity during the spring bloom in Newfoundland coastal waters. *Science* 233, 359–361.
- Porter, K.G., Feig, Y.S., 1980. The use of DAPI for identifying and counting aquatic microflora. *Limnol. Oceanogr.* 25, 943–948.
- Poulton, S.W., Raiswell, R., 2005. Chemical and physical characteristics of iron oxides in riverine and glacial meltwater sediments. *Chem. Geol.* 218, 203–221. <http://dx.doi.org/10.1016/j.chemgeo.2005.01.007>.
- Rignot, E., 2008. Changes in West Antarctic ice stream dynamics observed with ALOS PALSAR data. *Geophys. Res. Lett.* 35, L12505. <http://dx.doi.org/10.1029/2008GL033365>.
- Rochelle-Newall, E.J., Fisher, T.R., 2002. Production of chromophoric dissolved organic matter fluorescence in marine and estuarine environments: an investigation into the role of phytoplankton. *Mar. Chem.* 77, 7–21.
- Sanders, R.W., Caron, D.A., Berninger, U.G., 1992. Relationship between bacteria and heterotrophic nanoplankton in marine and freshwaters: an interecosystem comparison. *Mar. Ecol. Prog. Ser.* 86, 1–14.
- Schoof, C., 2010. Glaciology: Beneath a floating ice shelf. *Nat. Geosci.* 3, 450–451.
- Sedwick, P.N., DiTullio, G.R., 1997. Regulation of algal blooms in Antarctic shelf waters by release of iron from melting sea ice. *Geophys. Res. Lett.* 24, 2515–2518.
- Sherr, B.F., Sherr, E.B., Hopkinson, C.S., 1988. Trophic interactions within pelagic microbial communities: Indications of feedback regulation of carbon flow. *Hydrobiologia* 159, 19–26.
- Shields, A.R., Smith Jr., W.O., 2008. An examination of the role of colonial *Phaeocystis* Antarctica in the microbial food web of the Ross Sea. *Polar Biol.* 31, 1091–1099. <http://dx.doi.org/10.1007/s00300-008-0450-z>.
- Smith Jr., W.O., Gordon, L.L., 1997. Hyperproductivity of the Ross Sea (Antarctica) polynya during austral spring. *Geophys. Res. Lett.* 24, 233–236.
- Smith Jr., W.O., Marra, J., Hiscock, M.R., Barber, R.T., 2000. The seasonal cycle of phytoplankton biomass and primary productivity in the Ross Sea, Antarctica. *Deep-Sea Res. II* 47, 3119–3140.
- Stammerjohn, S.E., Martinson, D.G., Smith, R.C., Yuan, X., Rind, D., 2008. Trends in annual Antarctic sea ice retreat and advance and their relation to El Niño–Southern Oscillation and Southern Annual Mode variability. *J. Geophys. Res.* 113, C03S90.
- Stedmon, C.A., Markager, S., 2001. The optics of chromophoric dissolved organic matter (CDOM) in the Greenland Sea: An algorithm for differentiation between marine and terrestrially derived organic matter. *Limnol. Oceanogr.* 46, 2087–2093.
- Steinberg, D.K., Nelson, N.B., Carlson, C.A., Prusak, A.C., 2004. Production of chromophoric dissolved organic matter (CDOM) in the open ocean by zooplankton and the colonial cyanobacterium *Trichodesmium* spp. *Mar. Ecol. Prog. Ser.* 276, 45–56.
- Taylor, A.G., Landry, M.R., Selph, K.E., Yang, E.J., 2011. Biomass, size structure and depth distributions of the microbial community in the eastern equatorial Pacific. *Deep-Sea Res. II* 58, 342–357.

- Thoma, M., Jenkins, A., Holland, D., Jacobs, S., 2008. Modelling Circumpolar Deep Water intrusions on the Amundsen Sea continental shelf, Antarctica. *Geophys. Res. Lett.* 35, L18602. <http://dx.doi.org/10.1029/2008GL034939>.
- Thuróczy, C.-E., Alderkamp, A.-C., Laan, P., Gerringa, L.J.A., Mills, M.M., Van Dijken, G.L., De Baar, H.J.W., Arrigo, K.R., 2012. Key role of organic complexation of iron in sustaining phytoplankton blooms in the Pine Island and Amundsen Polynyas (Southern Ocean). *Deep-Sea Res. II* 71–76, 49–60.
- Urban-Rich, J., McCarty, J.T., Fernandez, D., Acuna, J.L., 2006. Larnaceans and copepods excrete fluorescent dissolved organic matter (FDOM). *J. Exp. Mar. Biol. Ecol.* 332, 96–105.
- Williams, W.J., Carmack, E.C., Ingram, R.G., 2007. Physical oceanography of polynyas. In: Smith, W.O., Barber, D.G. (Eds.), *Polynyas: Windows to the World*. Elsevier, Amsterdam, pp. 55–85.
- Wilson, S.E., Swalethorp, R., Kjellerup, S., Wolvertson, M.A., Ducklow, H.W., Yager, P.L., 2015. Meso- and macro-zooplankton community structure of the Amundsen Sea Polynya, Antarctica (Summer 2010–2011). *Elem. Sci. Anth.* 3, 000033.
- Yager, P.L., Sherrel, R.M., Stammerjohn, S.E., et al., 2012. ASPIRE: The Amundsen Sea Polynya international research expedition. *Oceanography* 25, 40–53.
- Yang, E.J., Hyun, J.-H., Kim, D., Park, J., Kang, S.-H., Shin, H.C., Lee, S.H., 2012. Mesoscale distribution of protozooplankton communities and their herbivory in the western Scotia Sea of the Southern Ocean during the austral spring. *J. Exp. Mar. Biol. Ecol.* 428, 5–15.
- Zöllner, E., Hoppe, H.G., Sommer, U., Jürgens, K., 2009. Effect of zooplankton-mediated trophic cascades on marine microbial food web components (bacteria, nanoflagellates, ciliates). *Limnol. Oceanogr.* 54, 262–275.